

Emerging concepts for the dynamical organization of resting-state activity in the brain

Gustavo Deco*, Viktor K. Jirsa[†] and Anthony R. McIntosh[§]

Abstract | A broad body of experimental work has demonstrated that apparently spontaneous brain activity is not random. At the level of large-scale neural systems, as measured with functional MRI (fMRI), this ongoing activity reflects the organization of a series of highly coherent functional networks. These so-called resting-state networks (RSNs) closely relate to the underlying anatomical connectivity but cannot be understood in those terms alone. Here we review three large-scale neural system models of primate neocortex that emphasize the key contributions of local dynamics, signal transmission delays and noise to the emerging RSNs. We propose that the formation and dissolution of resting-state patterns reflects the exploration of possible functional network configurations around a stable anatomical skeleton.

Oxygen extraction
A quantitative medical imaging method to determine the regional consumption of oxygen in brain tissue.

*Institució Catalana de Recerca i Estudis Avançats (ICREA), Universitat Pompeu Fabra, Computational Neuroscience, Plaça de la Mercè, 10–12, 08002 Barcelona, Spain.

[†]Theoretical Neuroscience Group, Institut des Sciences du Mouvement UMR6233 CNRS, Marseille, France, and Center for Complex Systems and Brain Sciences, Physics Department, Florida Atlantic University, USA.

[§]Rotman Research Institute of Baycrest Centre, University of Toronto, 3560 Bathurst Street, Toronto, Ontario M6A 2E1 Canada.

Correspondence to G.D.

e-mail:

Gustavo.deco@upf.edu

doi:10.1038/nrn2961

The raison d'être of spontaneous brain activity has been debated for decades¹: does it have a functional purpose or is it merely an obstacle for brain function to overcome? Despite this uncertainty, modern neuroimaging practices often overlook spontaneous brain activity. Most studies have focused on changes in activity evoked by external stimuli, the response demands of a task or a cognitive challenge. The assumption in many of these studies was that ongoing activity is sufficiently random for it to be averaged out in statistical analysis. Indeed, this bias is evident in the labelling of imaging studies as 'activation' paradigms in which the experimental manipulation results in the activation of cerebral circuits that are necessary for performing the task. Implicit in this focus is the idea that one could describe these changes in relation to some ideal baseline state in which, presumably, brain activity is low. Hence, most of the published work has emphasized the brain areas that showed increases — or activations — relative to the putative baseline condition. However, it became clear that despite the most elegant experimental designs, there are consistent patterns of deactivation that often accompany increased cognitive demands. Several researchers began to examine these deactivations based on the idea that the low-level baseline tasks were active states and that the patterns of activation and deactivation represented a shift in the balance from a focus on the subject's internal state and ruminations to the external environment. This is

epitomized in Andreasen's suggestion that the 'rest' condition used as a baseline condition in many neuroimaging studies is better conceived as a state of Random Episodic Silent Thought². In a study of episodic memory, Nyberg *et al.*³ noted spatial patterns of deactivation with increasing cognitive load that were consistent across several studies in the literature at that time. Shulman *et al.*⁴, in a meta-analysis of position emission tomography (PET) data, also observed consistent deactivations with spatial patterns similar to those reported earlier (FIG. 1).

Following these observations, several researchers began studies of the metabolic profile of the brain with the goal to better understand the relationship between metabolic markers (for example, cerebral blood flow, oxygen extraction and BOLD fMRI) and the distribution of these markers during cognitive challenges. These studies converged on the observation that a set of regions with extraordinarily high metabolic rates (relative to other areas) seemed to be the regions that show the greatest deactivation during externally imposed cognitive challenges. This set of brain regions was labelled the default mode network (DMN) by Raichle and colleagues⁵. Much of the work that followed on the DMN suggested that this collection of regions subserves cognitive operations that are self-referential, a suggestion based on the observation that DMN regions overlap with regions that show activation in studies of self-referential behaviours^{6,7}, such as autobiographic memory and self-judgments^{8,9}. This

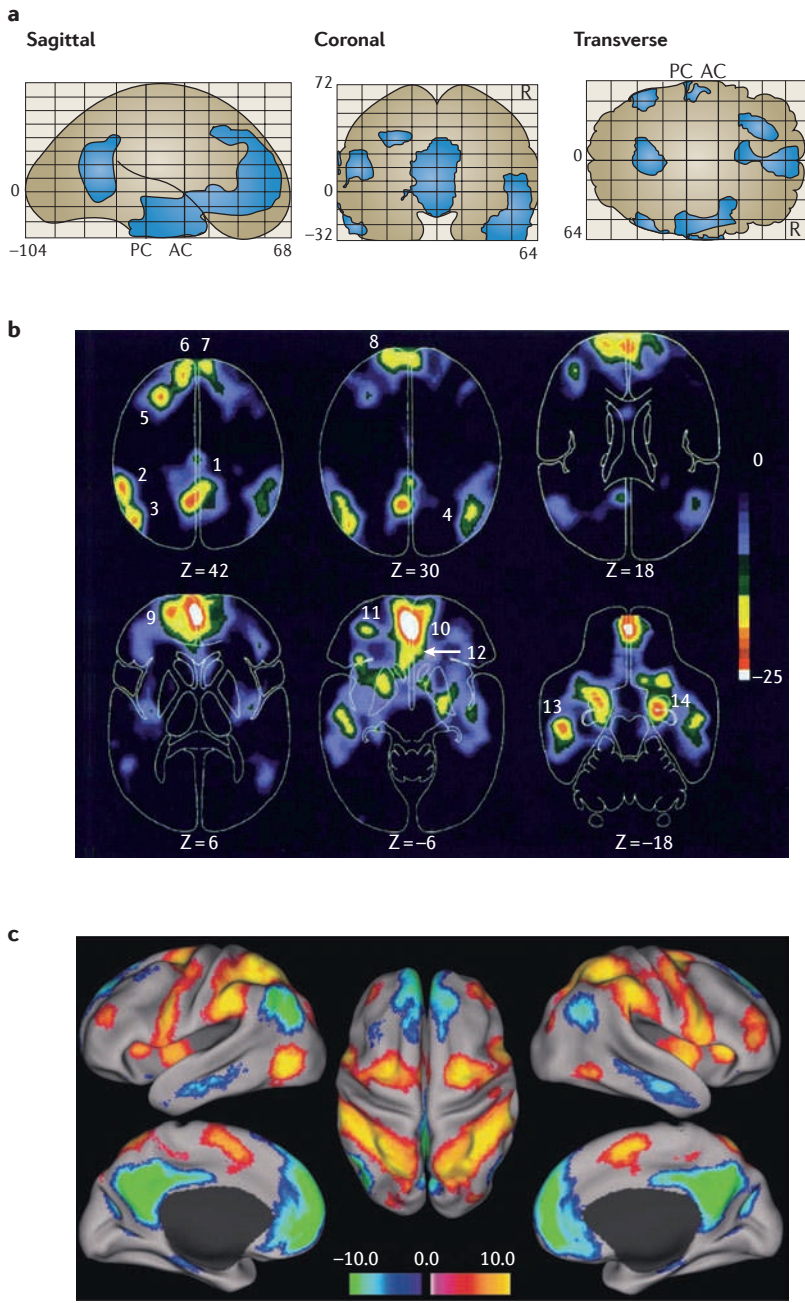


Figure 1 | The evolution of the default mode network in the neuroscience literature. **a** A 'glass brain' statistical map from a positron emission tomography (PET) study of regional cerebral blood flow (PET-rCBF) by Nyberg *et al.*³ showing areas of consistent activity reduction (deactivation, shown in blue) during episodic memory retrieval relative to a low-level baseline task. **b** | Axial sections showing a similar spatial map distribution of deactivations (a lighter colour indicates a greater deactivation, as shown by the bar on the right) in a meta-analysis of 9 PET-rCBF studies by Shulman *et al.*⁴ **c** | The results from an analysis of resting-state correlations in a functional MRI study by Fox *et al.*²³ Areas coloured red–yellow showed significant correlations with regions that are consistently activated during a demanding cognitive task (a task-positive network), whereas blue–green areas showed significant correlations with regions that are consistently deactivated during a demanding cognitive task (a task-negative network). The task-negative network is spatially similar to the 'default mode' network. Part **a** is reproduced, with permission, from REF. 3 © (1996) Society for Neuroscience. Part **b** is reproduced, with permission, from REF. 4 © (1997) MIT Press. Part **c** is reproduced, with permission, from REF. 23 © (2005) National Academy of Sciences. AC, anterior commissure; PC, posterior commissure; R, right.

notion has been challenged by studies of anaesthetized non-human primates that showed that the DMN persists during anaesthesia¹⁰ and the early stages of sleep^{11–13}, during which presumably no self-referential processes take place. This highlights an important problem regarding the putative connection between the DMN and self-referential behaviour, namely the problem of reverse inference^{14,15}: a certain cognitive operation may activate a brain region, but the activation of that brain region does not necessarily mean that the cognitive process is occurring. An extreme example of this is that although activation of the primary motor cortex (M1) is seen when someone moves their hand, the motor cortex may also be activated without an overt movement. It has been proposed that the functional relevance of activity in one brain region is determined by co-activation of other brain regions^{16,17}.

The observation that there are relatively consistent distributed patterns of activity during rest has led to the suggestion that it might be possible to characterize network dynamics without needing an explicit task to drive brain activity. This possibility has been explored in studies of resting-state networks (RSNs). Probably the first demonstration of an RSN using fMRI was the seminal paper by Biswal and colleagues¹⁸. They exploited the temporal fluctuations in the BOLD signal to examine the cross-correlation (that is, functional connectivity) between activity in M1 and that in other brain regions independently of any overt task. They noted a robust pattern of correlations with other motor regions, including the contralateral M1. Spatially, the functional connectivity pattern seemed to mimic the pattern of activation seen when subjects executed an overt motor response. Several subsequent studies also demonstrated that in the absence of an overt task, spontaneous fluctuations in the BOLD signal correlate across functionally related brain regions^{19–21}. Interestingly, some of these regions are also part of the DMN¹⁹. A more sophisticated study of resting-state patterns identified at least seven other independent networks of correlated activity that were robust across subjects²². In particular, regions within the DMN show tightly coherent activity over long time intervals but tend to show negative correlations with regions in which activity increases during a task ('task-positive regions'), such that as activity in DMN areas decreases, activity in task-positive areas increases²³ (for a recent debate on this issue, see REFS 24,25).

Thus, it is not understood what resting-state activity — or perhaps more broadly intrinsic activity dynamics — of the brain actually reflects. It is clear that a simple mapping of intrinsic activity dynamics to a cognitive process is not possible, but at the same time, in disorders in which cognition is disrupted, the intrinsic activity dynamics seem also to be disrupted^{26–29}. Intrinsic activity dynamics may therefore reflect some aspects of the functional capacity of neural systems. In this Review, we discuss computational studies that demonstrate that local and global dynamics, signal transmission delay and noise are important contributors to the organization and activity of RSNs. These studies, we suggest, provide a testable framework for a better appreciation

BOLD fMRI

Blood oxygen level-dependent (BOLD) functional MRI (fMRI) is a relatively new neuroimaging tool to map activity in the brain *in vivo*. Signal changes are dependent on the relative changes in blood oxygen levels in the brain capillary beds.

Functional connectivity

The relationship between activity in two or more neural sources. This usually refers to the temporal correlation between sources but has been extended to include correlations across trials or different experimental subjects. Functional connectivity methods include estimation of correlation coefficients and coherence. The estimation cannot be used to infer the direction of the relation between sources.

Diffusion spectrum imaging
An MRI technique that is similar to DTI, but with the added capability of resolving multiple directions of diffusion in each voxel of white matter. This allows multiple groups of fibres at each location, including intersecting fibre pathways, to be mapped.

Graph theory

A branch of mathematics that deals with the formal description and analysis of graphs. A graph is defined as a set of nodes (vertices) linked by connections (edges). The connections may be directed or undirected. A graph provides an abstract representation of the system's elements and their interaction.

Small-world architecture
A term derived from graph theory estimation referring to a network that combines high levels of local clustering among nodes (to form families or cliques) and short paths that globally link all nodes of the network.

Diffusion tensor imaging
(Often abbreviated to DTI.) An MRI technique that takes advantage of the restricted diffusion of water through myelinated nerve fibres in the brain to infer the anatomical connectivity between brain areas.

of the function of intrinsic activity dynamics. We conclude by discussing how these dynamic elements may combine with task-driven activity to support effective information processing.

Anatomical connectivity and RSNs

RSNs reflect the anatomical connectivity between the regions in a network. Anatomical studies using diffusion spectrum imaging and principles of graph theory have revealed important details of such structural connectivity³⁰. The connections between areas of mammalian brain networks are organized according to small-world architecture, in which neighbouring nodes show more connections than nodes that lie further apart^{31,32}. Within this architecture, certain regions have been identified as 'hubs'. Conceptually similar to an airline hub, these are nodes with a comparatively high number of connections to the rest of the network³¹. Interestingly, the DMN seems to consist of a collection of hubs³⁰. Of all hubs, the posterior cingulate cortex (PCC) and precuneus have the highest connection density and this defines them as a structural core³⁰.

This structural organization seems to map onto the functional connectivity of the DMN. fMRI studies in combination with diffusion tensor imaging have been used to examine anatomical connections between the regions of the DMN that show correlated activity during rest, and this has identified three functionally related regions: the area comprising the PCC and precuneus, the medial prefrontal cortex (MPFC) and the medial temporal lobes (MTLs)³³. Specifically, white matter tracts connect the PCC and precuneus to the MPFC and MTL. However, there were no tracts connecting the MPFC to the MTL, suggesting that functional connectivity may be achieved through other means — for example, a subnetwork linked through indirect anatomical connections of these and other regions.

The use of fMRI and diffusion spectrum imaging has allowed a comprehensive evaluation of the structure–function map of RSNs³⁴. This has shown that although structural connectivity is a good predictor of functional connectivity — if there is a direct anatomical connection, there is a functional connection — the opposite is not necessarily true; robust functional connectivity has been observed in the absence of a direct anatomical link (see also REF. 35). Furthermore, the within-subject test–retest reliability of functional connectivity was surprisingly low³⁴, and lower than one would expect if the patterns were solely anatomically determined. Intriguingly, low reliability was also found in a computational model of a structural architecture that was similar to the architecture suggested by empirical data. This suggests that within a stable anatomical skeleton there is some reconfiguration of functional networks.

To summarize, there is a consensus from the empirical data that functional connections persist without obvious external stimulation. It is also clear that there seem to be replicable spatial patterns of functionally connected networks that are somewhat independent of each other. What is missing is an explanation of why these patterns exist. Some accounts have interpreted the

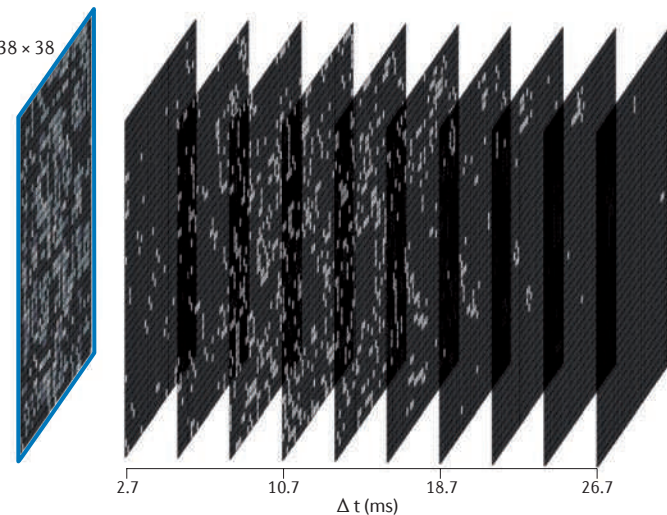
DMN from a cognitive point of view as representing networks involved in introspection^{6–8}. However, such a cognitive interpretation is difficult to uphold in light of the observations that these patterns also exist in the absence of consciousness during anaesthesia and sleep. We propose that it is more appropriate to link brain dynamics at rest to a constant inner state of exploration, in which the brain generates predictions about the likely network configuration that would be optimal for a given impending input. Metaphorically speaking, the resting state is like a tennis player waiting for the service of his or her opponent. The player is not static, but continues to move with small lateral jumps left and right to be able to react more effectively to the impending serve. Specifically, we propose a concept in which resting-state patterns are generated within a framework that is constrained by the underlying structural architecture, the variable time delays in signal transmission because of the differing distances between brain regions (for example, long- versus short-range connections) and the dynamics arising from local interactions among cells within a region. We examine this proposal using large-scale neural network simulations.

The missing link: dynamics

As discussed above, spontaneous brain activity during wakeful rest is not random but displays specific features, including the slow fluctuating spatiotemporal patterns in BOLD signals. Understanding how this activity emerges during rest is not a trivial problem. In complex dynamical systems like the brain, the collective outcome of system-wide dynamics is difficult to predict. This is true even when all major factors that are known to contribute to brain dynamics (for example, cortical–cortical connectivity, local cortical dynamics and intracortical connectivity) are assumed.

To fully understand the origin and function of spontaneous resting activity, we need to consider theoretical and computational models that enable us to study the link between anatomical structure and RSN dynamics. We consider in detail three models^{36–38} that explicitly propose a biological mechanism for the emergence of the spatiotemporal dynamics of the RSN. Other subsequent spatiotemporal modelling approaches^{39,40} can be understood in the same terms. A more microscopic approach was taken by Izhikevich and Edelman⁴¹ who used diffusion tensor imaging (DTI)-based connectivity for their large-scale network modelling and implemented single neuron models (rather than neural population models). This approach renders the network very high-dimensional compared to the population-based RSN models discussed here, and it requires the use of certain computational constraints (such as truncation of time delays and scaling down of the network size) to keep the numerical implementation efficient. It is not clear to what degree these constraints affect the simulated RSN dynamics. The microscopic approach has the natural advantage of allowing more detailed insights into the microcircuitry within brain regions and their involvement in the RSN dynamics for a given parameter setting. However, the high dimensionality deters one from performing

Box 1 | Space-time structure of couplings



The dynamics of a network are determined by the intrinsic dynamics of the network nodes (that is, the dynamics of a node in the absence of any couplings) and the network couplings (which allow the communication between two nodes of the network). The communication within a network is time delayed, typically owing to signal transmission along axonal fibres between the network nodes. Dynamics of complex systems with time delays is an active field of research, among other reasons owing to the enormous increase in complexity that is introduced just by one single delay. These changes include, but are not limited to, changes in the stability of equilibria in networks and the generation of novel oscillatory network behaviours, including chaos. The generic evolution equations of a large-scale brain network are mathematically expressed as:

$$\dot{X}_i(t) = N(X_i(t)) + \sum_j W_{ij} S(X_j(t - \tau_{ij})) = N(X_i(t)) + \sum_j \int dt' W_{ij} \delta(t - t' - \tau_{ij}) S(X_j(t'))$$

where $X_i(t) = (x_1^1(t) x_2^1(t) \dots x_n^1(t))$ denotes the i^{th} population activity determined by the n time-dependent population variables $x_k^1(t)$ with $k = 1, \dots, n$ at a given point in time t . The nonlinear function $N(X_i(t))$ is the intrinsic dynamics of the network node i (BOX 2). W_{ij} measures the weight of the connection between nodes i and j . The communication between the nodes occurs via the nonlinear transfer function $S(X_j(t - \tau_{ij}))$, which represents the firing rate and is often taken to be sigmoidal. S can be sometimes modulated by $X_j(t)$, which we have omitted here in the argument of S , for simplicity of presentation. Generally S depends on the population activity $X_j(t - \tau_{ij})$ generated at an earlier point in time $t - \tau_{ij}$. The rate of change of the population activity at a given node i depends on the coupling to the incoming signal from the j^{th} node, which itself depends on the strength of the connections W_{ij} and the timing of the arriving signals measured by their time delays τ_{ij} . In conjunction, these two attributes define the space-time structure of the couplings expressed as $W_{ij} \delta(t - t' - \tau_{ij})$ where $\delta(t - t' - \tau_{ij})$ is a delta function. The space-time structure of the couplings is graphically depicted in the figure, which illustrates the distribution of connection weights in the space spanned by the two connected areas and the time delay involved. This space-time structure of couplings has been used by Ghosh *et al.*³⁷ and Deco *et al.*³⁸ The greyscale code indicates the strength of connections, ranging from weakest (shown in black) to strongest (shown in white). The data are taken from the CoCoMac database and have been extrapolated to the human. For a velocity of 1 m per s the mean time delay is around 70 ms. This is a low estimate, as the distances used to compute the delay between two nodes are taken to be the Euclidean distances in physical space. Realistic fibres do not follow the shortest distance between two nodes and hence will be longer, with increased associated delays. In the absence of detailed knowledge of the space-time structure of the couplings, a common assumption in the large-scale brain modelling literature is to assume that the connection weights W_{ij} decay and the corresponding time delays increase as a function of physical distance^{74–79}. Other proposals for ways to approximate the space-time structure of the couplings include absorbing the effects of time delays in the rise and decay times of the network nodes⁸⁰ or approximating them as instantaneous³⁶. The latter approximation corresponds to a projection of the elements in the space-time structure to the plane with a time delay equal to zero. Neither of these approximations have been validated rigorously. Figure is reproduced from REF. 37.

systematic parameter searches to help understand the mechanisms of the RSN dynamics. Other models of RSNs^{42,43} do not explicitly address the spatiotemporal nature of the RSN, but rather focus exclusively on the temporal patterns, in particular the emergence of the ultraslow (<0.1-Hz) timescale. Hlinka and Coombes⁴² proposed a mechanism for generating slow oscillations that is based on the release of endogenous cannabinoids and on the retrograde volume signalling in synaptically coupled networks of excitatory neurons. Steyn-Ross and Steyn-Ross⁴³ demonstrated that neural field models may exhibit the emergence of ultraslow modulations of physiological activity when two instabilities (Hopf and Turing) interact nonlinearly. As neither of these models considers the spatial structure that underlies the RSN distribution, they shall not be further considered in this Review. The three following models address the characteristic spatial and temporal structure of RSNs observed in empirical data and use realistic neuroanatomical information from the macaque cortex provided by the CoCoMac neuroinformatics tool^{44,45}. To allow for approximate mapping of the human brain, the models used coarse cortical parcellation of 38 (REFS 37,38) or 47 (REF. 36) regions⁴⁶ to cover one hemisphere of the cerebral cortex.

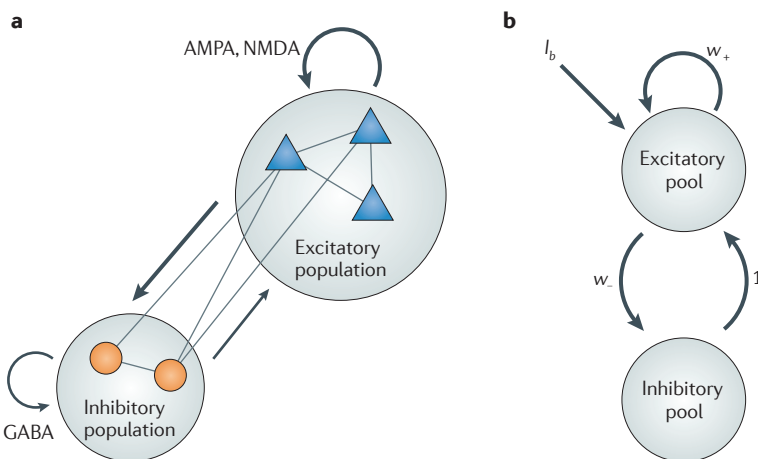
Anatomical and dynamical bases for RSN models

The three models we consider here start from the basic assumption that anatomical connectivity is a crucial factor in sculpting the global network dynamics. The first model³⁶ was the most straightforward test of this. Here, highly nonlinear dynamics were placed at each node of a cortical connectivity matrix. The second and third models^{37,38} were a more explicit test of the full space-time structure of the network couplings (BOX 1) connecting the local models of cortical areas (BOX 2). In the second model³⁷ the anatomical structure was refined by including time delays between network nodes. In addition, this model included effects of transmission velocity, connection strength and noise. The third model³⁸ included the same anatomical architecture and local dynamics, but explored a different parameter range and mechanism, giving rise to patterns of RSN dynamics. Below, we discuss the three models in more detail and then summarize them together to highlight the key insights they provide collectively.

Model 1. Honey *et al.*³⁶ proposed that the coherent fluctuations of resting-state activity reflect interactions between the local dynamics through anatomical connections of a small-world organized network^{31,32}. In this model a chaotic oscillator represented each brain region of the network. The coupling between oscillators was weak so as to generate transient synchronous activations between brain regions. This model did not include a time delay in signal transmission between brain regions, and therefore coupling between brain regions was instantaneous. Moreover, noise was not included in the simulations. Thus, the RSN dynamics in this model only consisted of the local dynamics of each node and instantaneous coupling.

First, functional connectivity was computed between all nodes over 240 s of simulated time. The pattern of

Box 2 | Local models of cortical areas



The global dynamics of the brain emerge from the collective dynamics of spiking neuronal networks. The global network is structured by the neuroanatomical connectivity matrix (BOX 1) that specifies how local spiking networks communicate with each other. At the local level of a brain area, the simplest assumption is to consider a network of interacting spiking neurons that are organized into a discrete set of populations (see the figure, part a). Populations are defined as groups of statistically similar excitatory or inhibitory neurons that share the same inputs and connectivity. A spiking neuron transforms a large set of incoming input spike trains from different neurons into an output spike train. Thus, at the microscopic level, neuronal circuits of the brain encode and process information through spatiotemporal spike patterns. One can assume that the dynamics of spiking neurons are properly captured by one-compartment, point-like models of neurons, such as the leaky integrate-and-fire (LIF) model⁸¹. In the LIF model, each neuron can be fully described in terms of a single internal variable, namely the depolarization of the neural membrane. The basic circuit of a LIF model consists of a capacitor in parallel with a resistor driven by a synaptic current (excitatory or inhibitory postsynaptic potential (EPSP or IPSP), respectively). When the voltage across the capacitor reaches a threshold, the circuit is shunted and a spike is generated and transmitted to other neurons.

In the brain, local neuronal networks comprise a large number of neurons that are massively interconnected. The dynamics can be properly described by a set of coupled differential equations corresponding to a LIF model for each neuron. Direct simulations of these equations yield a complex spatiotemporal pattern, covering the individual trajectory of the internal state of each neuron in the network. These types of direct simulations are computationally expensive, making it very difficult to analyse how the underlying connectivity relates to various dynamics. One way to overcome these difficulties is by adopting the population density approach, using the Fokker–Planck formalism⁸². In this approach, individual integrate-and-fire neurons are grouped together into populations of statistically similar neurons. A statistical description of each population allows for the derivation of a differential equation that describes the dynamical evolution of the averaged activity of a pool of equivalent neurons. Assemblies of motor neurons and the columnar organization in the visual and somatosensory cortex are examples of these pools. In a neuronal pool, the mean activity captures the time course of the firing rate and is determined by the proportion of active neurons — by counting the number of spikes in a small time interval t and dividing by the number of neurons in the pool and by t . Spikes are generated by a threshold process.

Assuming the population density approach, we can reduce the description of the dynamics of a local circuit of excitatory and inhibitory neurons by using the mean-field equations that describe the evolution of the population activity of an excitatory and an inhibitory pool. This yields the Wilson–Cowan model for a single brain area⁸³ (see the figure, part b), given by:

$$\dot{E}(t) = -E(t) + S(I_b + w_+ E(t)) - I(t) + n(t)$$

$$\dot{I}(t) = -I(t) + S(w_- E(t)) + n(t)$$

The excitatory population activity is denoted by $E(t)$ and the inhibitory by $I(t)$. S is again the sigmoid function, I_b some diffuse unstructured background activity, w_+ and w_- connection strengths and $n(t)$ is noise. These equations define the intrinsic dynamics as discussed in BOX 1.

To account for more complex dynamics beyond the modulation of the firing rate, more elaborate mode decomposition techniques have been developed^{84,85}. These approaches acknowledge the fact that not all neurons are statistically similar — that is, there is a parameter diversity (for example, different thresholds) among the neurons, which leads to the formation of functional clusters of similar dynamics within the population. The decomposition of the population activity into modes (corresponding to a functional cluster) allows for explicit evolution equations for the neural population activity from the microscopic neuronal equations. This set of coupled population equations reproduces the repertoire of the spatiotemporal population dynamics, including dynamic phenomena such as full synchronization, anti-phase clustering and oscillator death. AMPA, α -amino-3-hydroxy-5-methyl-4-isoxazole propionic acid; GABA, γ -aminobutyric acid; NMDA, N-methyl-D-aspartate.

Neural field

Values of neural activity that are defined over a continuous physical space, typically the two- or three-dimensional cortical sheet.

Transient

In dynamical systems this refers to time-dependent states evolving towards an attractor.

functional connectivity over this time window largely reproduced the structural connectivity between nodes. Interestingly, regions with a high degree of anatomical connectivity tended to also show a high degree of functional connectivity. At smaller time windows however, shorter-lived patterns of functional connectivity emerged that were not predicted by the anatomy. This observation shows that functional connectivity patterns depend on the timescale over which the correlations are calculated.

To more closely align the dynamics of model 1 with actual neuroimaging data, the oscillations for each node were converted to a BOLD signal using the Balloon–Windkessel haemodynamic model⁴⁷. The local BOLD signal and the strength of functional connectivity were computed over a long timescale of several hundred seconds. Two anticorrelated clusters of brain regions were identified that were similar to the pattern reported in the fMRI neuroimaging literature²³ (FIG. 2). Finally, the variation of BOLD signal at a given node was also related to the synchronous oscillations of that node with other nodes. In conclusion, in this model, resting-state activity patterns result from cluster synchronization between nodes, and different clusters correspond to different RSNs. The irregularity introduced by the chaotic character of the local and global dynamics is responsible for the alternating synchronization and desynchronization of the different RSNs.

Model 2. Ghosh *et al.*³⁷ proposed that the space–time structure of the network couplings (BOX 1) defines the dynamic framework for the emergence of resting brain fluctuations. Thus, unlike model 1, this model attempted to better represent the anatomical connectivity. To achieve a more precise estimate of cortico-cortical distances, connectivity data from tracer studies collated in CoCoMac were transformed to a regional map of human brain equivalents⁴⁶. The centre coordinates of the 38 cortical areas were calculated and their distances obtained from the geometry defined in the anatomical automatic labelling (AAL) cortical surface template of a human hemisphere⁴⁸. Regional dynamics were modelled as oscillators with a constant level of noise. Assuming a uniform transmission velocity, the approximate delays between each connected region were expressed as a function of their Euclidean physical distance divided by the velocity. The parametric manipulation of velocity tested the role of transmission delays between two different brain regions. After signal transmission delays, the second relevant parameter is the overall coupling strength. In this model, varying the levels of coupling strength resulted in scaling of all connection strengths within the network.

Ghosh *et al.*³⁷ systematically studied the stability of the network's equilibrium state (that is, the tendency to be in a state of quiescence) as a function of transmission delay and coupling strength. Characteristic time series with and without noise are shown in FIG. 3a. The stability diagrams (FIG. 3b) identify stable and unstable regions of quiescent and oscillatory dynamics, as well as the critical line separating regions of stability from instability. In stable regions, the network is at equilibrium, while the noise inherent in the system constantly drives the

network away from its stable equilibrium point. To be able to express its global noise-driven spatiotemporal characteristics, the network must operate sufficiently close to the critical line — that is, at the onset of oscillatory instability — otherwise the oscillatory return will be suppressed. In the presence of noise (the noise drive) and when close to the onset of oscillatory behaviour (the critical line), the network intermittently displays ~10-Hz oscillations (the oscillatory return), generating the well-known spindle-like characteristics of physiological measurements, including electroencephalography (EEG) and magnetoencephalography (MEG). The noise drive, the critical line and the oscillatory return are the crucial elements of the resting-state-generating mechanism in model 2. As the network attempts to return to its equilibrium, it displays intermittently characteristic oscillations until another ‘noise kick’ drives it away again. The neighbourhood of the equilibrium point is composed of the set of network behaviours that are shaped by the space–time structure of the couplings. The ongoing interplay between noise drive and oscillatory return leads to sampling and exploration of the brain's dynamic repertoire (FIG. 3a).

Indeed, when implemented in an anatomically accurate large-scale model with a biologically realistic range of transmission velocities, the dynamic repertoire is expressed by the transient activation of subnetworks and accompanying cortical wave dynamics (FIG. 3c). The travelling waves of neural activity in the alpha range propagate through the brain network, and the amplitude of these waves is modulated stochastically, manifesting the slow 0.1-Hz fluctuations. As such, the fast timescale can be considered to be the frequency of the carrier wave, whose amplitude modulation correlates with the resting-state fluctuations in the BOLD signal. The dynamic characteristics of the activity propagation, including the sequential activation of network nodes and the propagation speed, are determined by the space–time structure of the couplings. These constraints prescribe preferential paths through the network, which set the dynamic repertoire of the brain.

When the BOLD signal is computed, these subnetworks reflect the topography of RSNs with parietal, prefrontal and cingulate network components. As the transmission velocity is varied outside of the biologically realistic range, the space–time structure of the couplings changes: as a consequence the resulting transiently activated subnetwork disintegrates and the global pattern reorganizes. To perform a more quantitative test of the functional connectivity, Ghosh *et al.*³⁷ tested their simulations against the data of Fox *et al.*²³, who chose six predefined regions and computed the correlations against the other regions. All cross-correlations, except those between the frontal eye fields (FEFs) and the intraparietal sulcal cortex (PCIP), showed good correspondence between experimental and simulated data. As the transmission speed was scaled up towards infinity, the cross-correlation structure broke down. These findings again underscore the importance of time delays in the emergence of large-scale network dynamics expressed in RSNs.

Balloon–Windkessel haemodynamic model

A dynamical model in which neural activity (the BOLD signal) is transduced into brain perfusion changes. In this model, the BOLD signal is taken to be a static nonlinear function of normalized total deoxyhaemoglobin voxel content, normalized venous volume, resting net oxygen extraction fraction by the capillary bed and resting blood volume fraction.

Stability

In dynamical systems refers to a state that, if it is perturbed, will return after a time to the same configuration.

Instability

In dynamical systems refers to a state that, if it is perturbed, will escape away from the original configuration.

Carrier wave

A wave of a higher frequency that is modulated with another signal of a lower frequency, typically for the purpose of conveying information.

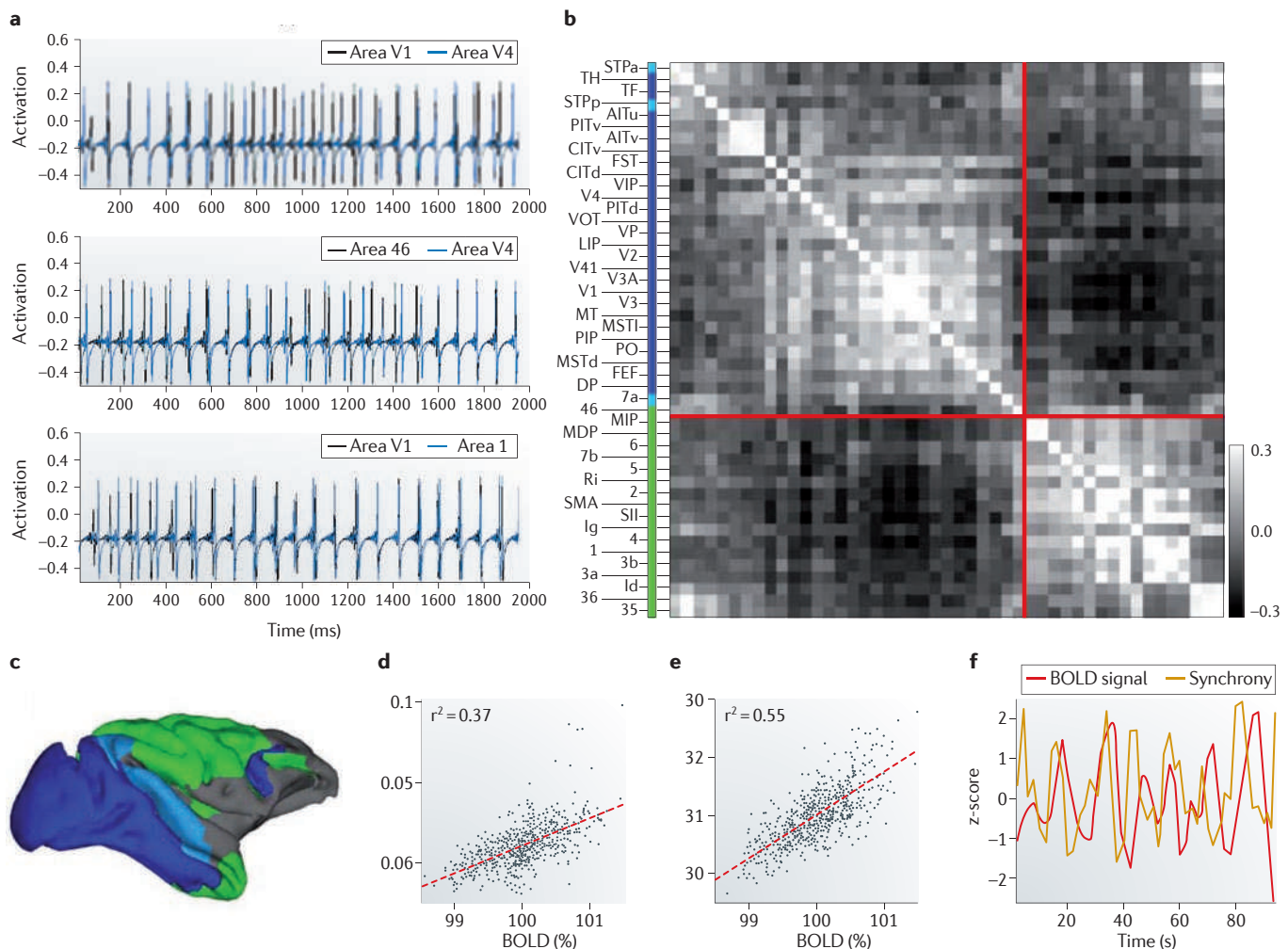


Figure 2 | Resting-state dynamics reflect interactions of the local dynamics through anatomical connections. **a** Basic mechanism of the Honey *et al.* model³⁶. The model simulates chaotic local neuronal dynamics in a network of inter-regional connections of the macaque neocortex. In this model, resting-state networks are caused by synchronization of nodes in clusters owing to the underlying small-world organization of the neuroanatomical structure. In each panel, the two traces show the characteristic chaotic time course of activity of neural populations in two particular areas. Synchronization (overlapping of the two traces) and desynchronization evolve on a slow timescale (<0.1 Hz), whereas neural oscillations evolve on a faster timescale (~10 Hz). The transient synchronization of neural populations is closely correlated with the ultraslow fluctuations in the BOLD signal. Parts **b–f** show estimated BOLD signals and their relation to synchrony. **b** A BOLD correlation matrix, computed from an estimated BOLD time series (after regressing out global BOLD fluctuations) in which BOLD activity was sampled every 2 s. **c** A correlation map obtained using areas V4 and SII as seed regions. Brain regions in which BOLD activity positively correlated with activity in V4 are shown in blue, and regions in which activity positively correlated with activity in SII are shown in green. Regions that did not show positive correlations or that positively correlated with both seed regions are shown in light blue. **d** A scatter plot of the global BOLD signal against variations in aggregate network transfer entropy. This reveals that fluctuations in the BOLD signal and functional connectivity that occur over many seconds are related to one another. **e** A scatter plot of the global BOLD signal against variations in synchronization. Synchronization is measured as the percentage of phase-locked time steps (in-phase or anti-phase) across all node pairs. This reveals that fluctuations in the BOLD signal and functional connectivity that occur over many seconds are related to the fast synchronization dynamics of the system. **f** BOLD signal and synchrony shown over a 95-s data segment recorded from area 7a. Synchrony is calculated as the total time that area 7a is phase-locked with any of the other nodes in the large-scale network.

Model 3. Let us now consider the third scenario in the model of Deco *et al.*³⁸ (FIG. 4a). As in Ghosh *et al.*³⁷, the main idea was that complex network dynamics emerge from the interactions of simple local dynamics with the effects of connectivity, time delays and noise, but in this model the levels of noise fluctuations were investigated

parametrically. The fast dynamics of local oscillations in the (40-Hz) gamma range were expressed as Wilson–Cowan population rate models (BOX 2). In particular, the Wilson–Cowan model is tuned in such a way that each independent node, if disconnected, is silent (low activity regime). However, because their working point is very

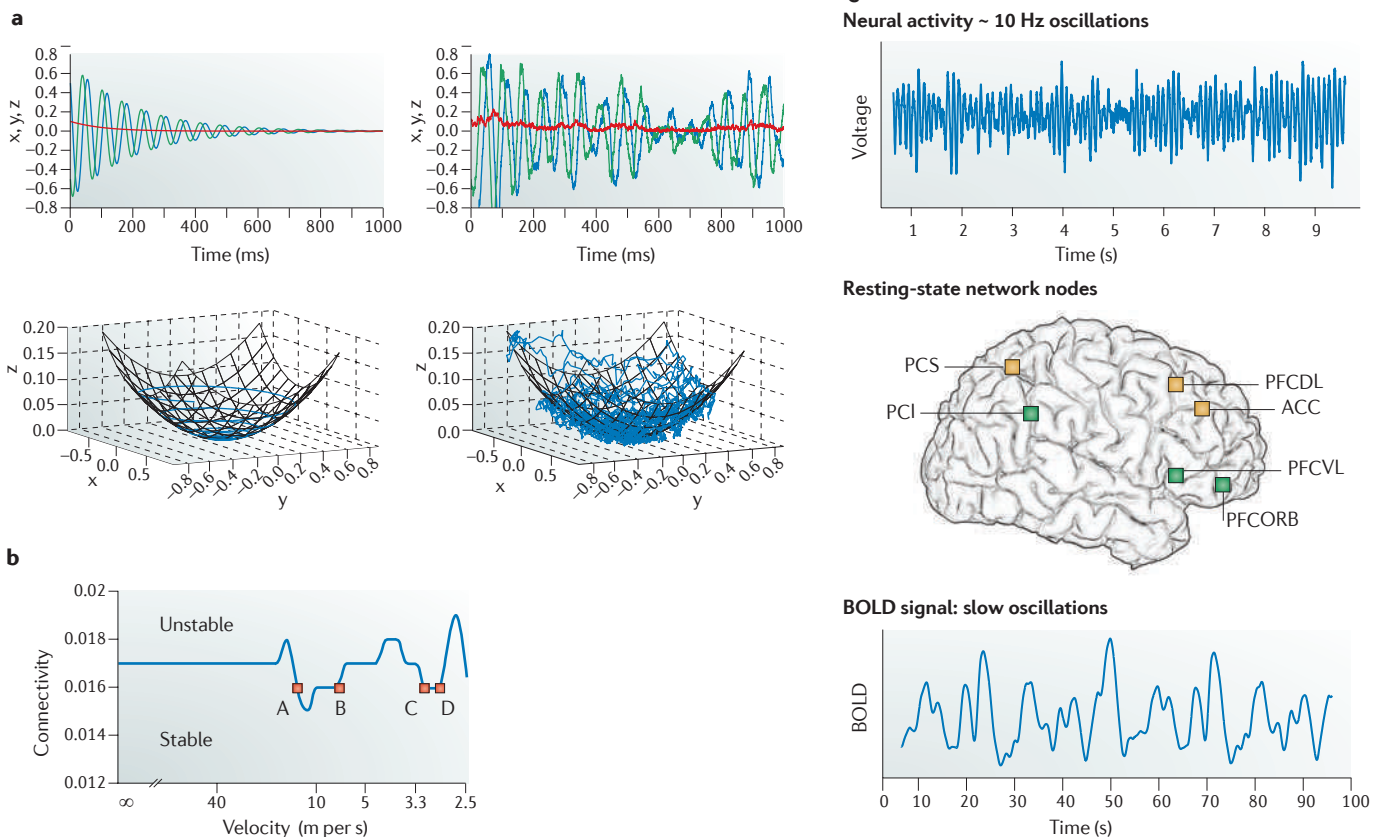


Figure 3 | Resting-state networks emerge from a dynamic framework of noise, anatomical connectivity and time delays. **a** Basic mechanism of the Ghosh *et al.* model³⁷. This model proposes that the synchronizations within the network are mutually determined by the large-scale connectivity and the transmission delays along connections. When noise drives the network out of equilibrium, the subsequent relaxations establish the resting-state dynamics. To illustrate this stochastic mechanism, we computationally solve a dynamic system of three variables with a stable equilibrium point. The trajectories approach the stable equilibrium in the absence of noise by spiralling down a paraboloid (lower left panel). The corresponding time-series of two variables display a damped oscillation (upper left panel; shown in green and blue), whereas the third variable (shown in red) relaxes to zero in a non-oscillatory fashion (upper left panel). In the upper right panel, the same dynamic system is computationally solved in the presence of noise. Driven by the noise, the system explores the neighbourhood of the equilibrium point — here, the paraboloidal manifold (lower right panel). Each excursion further away from the equilibrium is followed by an oscillatory return along the paraboloid, giving rise to intermittent, fast neurophysiological oscillations at 10 Hz (upper right panel). **b** | The stochastically driven exploration of the dynamic neighbourhood of an equilibrium is predominant at the edge of the onset of oscillatory behaviour. The critical line demarcating this oscillatory onset is plotted as a function of axonal transmission speed (velocity) and coupling strength (connectivity). Points A, B, C and D identify biologically relevant velocity ranges close to the critical line, with B and C defining the upper and lower ranges, and A and D the ranges beyond. **c** | Representative time courses for the neural signal (upper panel) and BOLD signal (lower panel) are shown for the same node (orbital prefrontal cortex; PFCORB). In the middle, the dominant network nodes of the two subnetworks in the Ghosh *et al.*³⁷ model were identified using principal component analysis and are shown in green and yellow. The subnetworks span the space in which the majority of the resting-state dynamics takes place, and correspond to the subspace in FIG. 3a in which the paraboloid is defined. ACC, anterior cingulate cortex; PCI, inferior parietal cortex; PCS, superior parietal cortex; PFCDL, dorsolateral prefrontal cortex; PFCVL, ventrolateral prefrontal cortex. Part **b** is reproduced from REF. 37.

Hopf bifurcation

In nonlinear dynamics, a local bifurcation in which an initially stable fixed point of a dynamical system loses its stability in an oscillatory fashion.

near to a Hopf bifurcation (BOX 2), when nodes are coupled, each node starts to oscillate. The parameters were chosen such that the oscillation of each node — arising from the coupling — is in the gamma band range of 40 Hz. Hence, in this model, complex collective brain dynamics emerge from the couplings between simple oscillators rather than from the complexity of the local dynamics (in this sense it differs from model 1). Note that a 40-Hz fast oscillation at the local brain area level

enables one to study the potential link between fast local dynamics and slow global fluctuations^{49,50}.

The network dynamics were obtained by coupling single nodes using the connectivity matrix with an identical space–time structure as that used in model 2. Model 3 showed that for particular transmission velocities (v), cluster synchronization patterns emerged — that is, certain groups of brain areas showed more synchronization than others. The synchronous groups of brain

areas divided the network into two clusters (similar to the ones found in model 1). FIGURE 4b shows that the synchronization level is relatively low for most of the velocity values except for two regions that show elevated levels of synchronization. The left peak at ~1.5 m per s corresponds to one of the clusters, and the right peak at ~2.0 m per s to the other cluster.

In the area of the graph between the two synchronization clusters ($v = 1.65$ m per s), maximum synchronization of the system is expected to alternate between one and the other cluster because of the underlying fluctuations. In fact, at this point a stochastic resonance⁵¹ effect exists — that is, an optimal level of noise that drives transitions between the two multistable states of synchronization in one cluster. Furthermore, at that optimal level of noise, ultraslow oscillations at the global level and anticorrelation between the different RSNs emerge (FIG. 4c). The figure shows that the model can reproduce both the slow 0.1-Hz oscillations and the anticorrelation of the BOLD signals of both clusters. FIGURE 4d shows how the resting-state features are completely distorted, or even disappear, if the transmission delays are removed.

The fact that synchronization predicts BOLD activity is not trivial. These results mean that there is a coupling between the degree of synchronization and neural activity that is manifest in elevated BOLD signals. This coupling has been studied in the context of evoked responses⁵² and in terms of endogenous fluctuations⁵³. These analyses of simulated spike trends and local field potentials show that in nearly every domain of parameter space, mean activity and synchronization are tightly coupled. This suggests that indices of brain activity that are based purely on synaptic activity (for example, fMRI) may also be sensitive to changes in synchronous coupling. Thus, these simulations explain why BOLD might be particularly sensitive to slow fluctuations in fast, synchronized dynamics.

A related set of earlier models sharing a similar outcome in the relationship between brain-like network topology and local and global network dynamics are those developed by Zhou *et al.*^{54,55}. In their models, the authors studied the emergence of global spatiotemporal patterns using realistic neuroanatomical connectivity matrices (from cats and macaques), ignoring the delay in the communication between different nodes. They demonstrated that the use of a simple oscillatory neural mass model for the local node dynamics results in very simple global patterns, namely full synchronization, which is inconsistent with the activity patterns found in the resting state. However, when they replaced the local node dynamics with a hierarchical recurrent network of excitable neurons with typical small-world topology (which accounts for the basic features of realistic local neuronal connectivity at the cellular level), the simulations of this ‘network of networks’ could generate biologically plausible global dynamical patterns. As in the case of Honey *et al.*³⁶, the global, structured fluctuation characteristics of the resting state result from the use of a complex model (a small-world recurrent model in the case of Zhou *et al.*⁵⁶, and a chaotic model in the case of Honey *et al.*³⁶) at the node level, because in the absence of time delays,

simpler models generate trivial global behaviour. Let us remark at this point that networks of coupled simple oscillators have been studied in physics⁵⁷. In general, networks of oscillators show — in the absence of delays — trivial global dynamics, namely full synchronization^{57,58}, whereas more complex dynamics emerge if delays and noise are introduced, as in the models by Ghosh *et al.*³⁷ and Deco *et al.*³⁸. A similar noise-driven multistability as in Deco *et al.*³⁸ has been proposed and was studied at the local level of brain areas to account for ongoing spontaneous activity at the cellular level⁵⁹. At the microscopic level, Arieli *et al.*⁶⁰ first showed that spontaneous activity (measured with optical imaging) is highly coordinated across large assemblies in anaesthetized cat primary visual cortex (V1), and that the pattern of co-activation is feature-specific in the sense that discharge of individual neurons is temporally locked to the activation of other cells with similar orientation preferences (resulting in orientation maps). Moreover, the variability in such ongoing activity can explain much of the variability in subsequent sensory-evoked responses, indicating a potential link with perception. Blumenfeld *et al.*⁶¹ accounted for this type of cellular ongoing activity by assuming that this activity resulted from noise-driven transitions between multistable attractors of the intracortical network. They suggested a rate model that was endowed with a simple local connectivity rule and showed that it yields attractor states that are highly similar to orientation maps that are alternatively activated in the absence of stimulation. They also considered the case in which the activity is evoked by a visual stimulus and showed how a structured afferent input can select the orientation map that matches the stimulus’ orientation. The model of Blumenfeld *et al.*⁶¹ therefore suggests that orientation maps are encoded in the lateral connections, and that these connections can generate orientation maps both when the activity is spontaneous and when it is evoked by a visual stimulus. In this sense, the model of Blumenfeld *et al.*⁶¹ (at the microscopic cellular level) and the model of Deco *et al.*³⁸ (at the global neuroanatomical level) propose that spontaneous ongoing activity is built up by multistable attractors (each one related to different specific tasks or stimulations) and that in the resting state it fluctuates through transitions between those attractor states owing to unstructured input — that is, noise.

Model summary. From the three models described above, several key outcomes are worth emphasizing. Across the timescales that are usually considered in fMRI, the pattern of RSNs is largely dependent on anatomical connectivity. Both the modelling and empirical work illustrate that the anatomical connections enable functional connections to emerge, but that a number of possible functional connectivity patterns can be expressed around the same anatomical skeleton. Moreover, as illustrated in model 1, the structure–function relation of an RSN across long timescales is strong, whereas numerous functional subnetwork configurations are possible at shorter timescales. The importance of anatomy, in terms of the presence of a connection and time delays, was more explicitly demonstrated in model 2.

Attractor

In dynamical systems refers to a set towards which a system evolves. Geometrically, this set may be a point, a curve or a manifold.

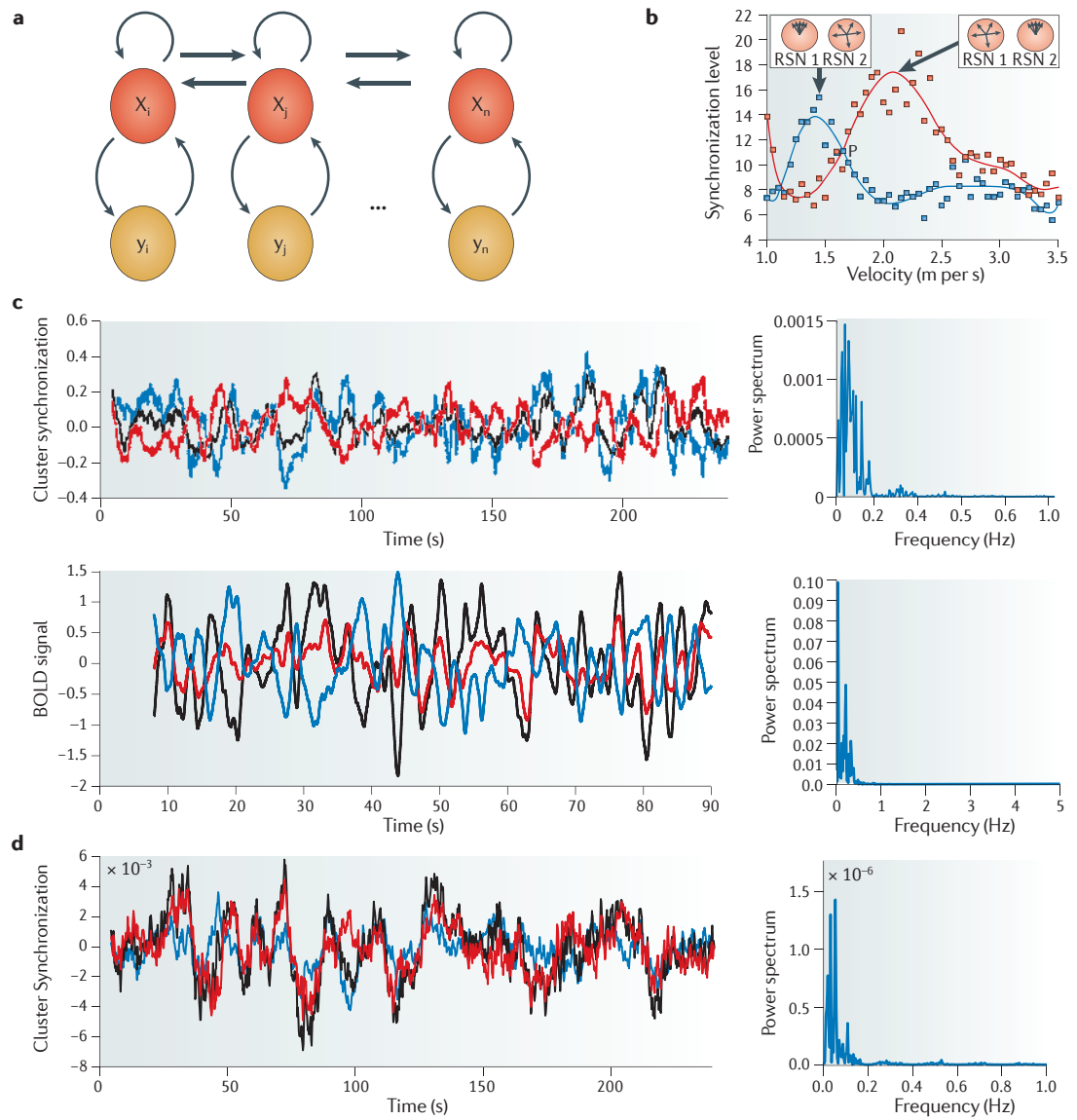


Figure 4 | Ultra slowly varying resting-state networks resulting from noise-driven transitions between multistable states. **a** Basic mechanism of the Deco *et al.* model³⁸. This model considers that resting-state ultraslow oscillations and the emergence of anticorrelated subnetworks result from noise-driven transitions between multistable states. In this scenario, multistable cluster synchronization states appear in coupled Wilson–Cowan oscillator systems owing to the delay of transmission times. This highlights the importance of the space–time structure of couplings in networks, in that the anatomical connectivity captures the spatial component and the transmission time delays the temporal component thereof. This scenario explicitly considers the link between local neuronal communication and global cortical dynamics, and in particular the interaction between fast local dynamics in the gamma range (40 Hz) and the ultraslow oscillations at the global level (0.1 Hz). The figure shows the network architecture built up by Wilson–Cowan units coupled through excitatory pools. Each node (i, j, \dots, n) corresponds to a Wilson–Cowan unit that expresses, through a mean-field-like rate model, the coupling between excitatory populations (shown by red circles) and inhibitory populations (shown by the yellow circles) of neurons.

b Level of synchronization in each of the two extracted clusters as a function of the transmission velocity. Two regions show elevated levels of synchronization that correspond to the increase in synchronization in either one of the community clusters: the left peak corresponds to one of the communities and the right peak to the other community. In the working point (P) between the two synchronization peaks ($v = 1.65$ m per s), the system is expected to alternate between one and the other cluster owing to the underlying fluctuations. **c** Temporal evolution of the network at the working point P. The temporal evolution of the synchronization level for each of the two individual communities (community 1, shown in black; community 2, shown in red; difference, shown in blue) is shown in the upper left panel, and the power spectrum of the signal given by differences between the levels of synchronization of both communities is shown in the upper right panel. The corresponding BOLD signals are shown in the lower left panel, and the power spectrum of the BOLD signal given by the differences between the level of BOLD signal between both communities is shown in the lower right panel. **d** Temporal evolution of the network when transmission delays are neglected. In this case, the ultraslow oscillations and the patterns of anticorrelations that are typical of the resting-state activity are completely distorted. RSN, resting-state network. Parts **c** and **d** are reproduced, with permission, from REF. 38 © (2009) National Academy of Sciences.

The role of the spatial and temporal structure was evident in that once they are considered within the constraints of an anatomically accurate framework, realistic network dynamics emerge only with the proper scaling of connection strength and conduction velocity. These dynamics represent intermittent metastable behaviour in which the system explores a number of potential functional network configurations — its dynamic repertoire. Importantly, the key nodes that seem to move the system towards this metastable state are the constituents of the DMN. Models 2 and 3 underscore the crucial contribution of ‘noise’ in the local node dynamics as the fuel to move the system to a metastable state. The contribution of noise was most clearly captured in model 3, in which exploration of dynamic repertoire showed the classic ‘inverted U’ stochastic resonance effect. Finally, all three models confirmed the presence of at least two networks whose temporal dynamics are anticorrelated. This observation supports the idea that the anticorrelations observed in the fMRI literature are probably not an analytic artefact²⁴. A crucial insight from the three models is that the anticorrelation does not arise from a direct antagonistic relation between networks, but rather embodies the different spatiotemporal structure of coherent networks in a larger anatomical skeleton.

Implications for measuring RSNs and the DMN

All three models make it clear that the dynamics of RSNs are accessible through most neuroimaging methods, particularly through fMRI. One obvious implication of model 1 is that functional network configurations depend on the time window over which these network dynamics are measured. Measurements over longer time windows recapitulate the anatomical connectivity, reflecting the RSNs that have been characterized in the literature, especially the DMN^{19,36}. Shorter time windows emphasize the small departure from the RSN pattern, in which different nodes form new functional networks for a short period of time and then return to the RSN pattern. Whether these excursions are accessible with fMRI is an open question, but it is clear that functional dynamics of the brain span multiple spatial and temporal scales. This observation also emphasizes the crucial link between space and time, such that the picture one derives of the constituents of a network depends greatly on the time window over which the dynamics are assessed. There is little doubt that the anatomical connectivity provides the conduit that enables the formation of functional networks, but structure and function are not isomorphic³⁴. The models we have reviewed here, as well as other, related studies^{55,62}, suggest a certain degree of caution is warranted in holding too strongly to the notion that there are a certain number of ‘functional networks’. It is more likely that the deterministic structure provided by the anatomy allows for certain functional networks to be repeated frequently in time, but that at any given point the precise configurations depend on the part of the dynamic repertoire that is being explored (that is, intrinsic activity) and the impact of the environmental demands (for example, of the task).

Metastability

In dynamical systems refers to a state that falls outside the natural equilibrium state of the system, but that persists for an extended period of time.

The three models express slightly different aspects of the relationship between fast and slow oscillations in brain networks. In the scenario of Ghosh *et al.*³⁷ (model 2), travelling waves of neural activity in the alpha range propagate through the brain, expressing the slow 0.1-Hz fluctuations through amplitude modulations. The link between the fast and slow oscillations in the models of Honey *et al.*³⁶ and Deco *et al.*³⁸ (models 1 and 3) is different from model 2. First, there is no amplitude modulation of a carrier wave and the networks oscillate with approximately constant amplitude in the alpha and gamma ranges, respectively. Instead, the neural signals display transient synchronization of neural population clusters, which will also find its expression on the scalp level in EEG or MEG. In models 1 and 3, the shift of synchronization from one cluster to the other generates scalp topographies that, when considered across time, mimic a travelling wave with a carrier frequency in the alpha and gamma range. This travelling wave propagates across the scalp with a time period corresponding to the ultraslow frequency range of <0.1 Hz, whereas in model 2 the propagation speed is determined by the faster carrier frequency in the alpha range. Although the mechanisms relating the fast and slow oscillations proposed by the three models are not mutually exclusive, further insights will be generated by spatiotemporal analyses — that is, detailed quantitative spatiotemporal analyses of BOLD and encephalographic data will have to be employed to clarify to what degree these mechanisms are actually present and accessible in empirically measured resting-state dynamics.

Various concepts have emerged from these studies, illuminating the role of network coupling and noise in large-scale systems. When brain regions are coupled across large distances, the associated transmission delays are not negligible if the timescales of the observed dynamics and delays are similar. Then the network couplings have a space–time structure that shapes the resulting network dynamics by determining the form and geometry of a manifold and its flow in the state space of the system. As the network activity evolves in time, the associated trajectory follows the flow along the manifold. The flow and the manifold prescribing this evolution represent the deterministic features of the network dynamics. Exploring the dynamic repertoire illustrates the effects of noise and introduces a stochastic element into the network dynamics. Noise drives the network continuously out of its equilibrium, and the network responds by moving towards its equilibrium following the deterministic flow on or towards the manifold. This continuous interplay of stochastic and deterministic components generates the perpetual transient dynamics with its intermittent oscillatory features characteristic for the resting state. It is intriguing that the stochasticity can express itself only if the deterministic framework of the network is critical — that is, close to instability^{37,38}. The instability itself may not have a direct functional role, though indirectly its presence is imperative in allowing the fluctuations to occur.

Conclusions and perspective

Modelling of RSNs shows that consideration of the interplay between sources of intrinsic variability of brain signal and the ensuing interplay with extrinsic sources is important. Some human developmental studies have suggested profound correlations between the emergence of 'brain noise' and cognitive stability^{63,64}, whereas in normal aging this intrinsic variability shows regional decreases that may impact behaviour⁶⁵. fMRI studies have demonstrated that the state of the intrinsic activity predicts trial-to-trial cognitive function^{66,67}. Bearing in mind these considerations and the results from the models that have been summarized here, we can now formally consider the role of noise and variability in the brain.

An optimal amount of noise seems to improve signal detection for a single neuron⁶⁸. At the level of full neural ensembles and large-scale networks, the direct effect of noise is less easy to define. Noise *per se* would be a property of local dynamics of cells and, potentially, of ensembles. At this level, the noise would be similar to random fluctuations (something that most researchers would intuitively consider to be noise), though it would probably have some deterministic structure and not be purely random. At the level of networks, noise in the absence of external stimulation drives the network dynamics, but the anatomical architecture provides the landscape within which different possible network configurations occur.

Brain networks generally possess a small-world construction, in which there are multiple ways for different network elements to interact. In the presence of noise, the system will visit these network configurations spontaneously. In this case, we speculate that the noise provides the kinetic energy for the network to explore possible functional architectures, which gives rise to variability in the measured network dynamics. It seems reasonable to link this behaviour to the notion from Bayes' models of the brain^{69,70}: by being in a constant state of exploration the brain generates predictions about likely future network configurations that will be appropriate for novel contexts. The variation in predictions is driven both by noise at the local level and by the range of available functional network configurations.

Although they were originally described through indirect and slow measures of neuronal activity (through BOLD fMRI), it is now clear that large-scale RSNs correlate with precise (yet incompletely described) neuronal rhythms at faster frequencies. The challenge for future models will be to answer the key question of how the resting state is expressed in the fast timescales measured electrophysiologically⁷¹. Studies in which brain activity is perturbed using transcranial magnetic stimulation (TMS) may be able to test the proposed mechanisms underlying the dynamics of the resting brain, by introducing perturbations to particular nodes and thereby biasing the competition among subnetworks. Studies in the developing brain may provide a new domain of exploration that might shed light on the change of intrinsic activity that accompanies structural maturation and experience^{6,72}. Finally, it may be possible to account for some of the age-related and pathology-related changes in cognitive function in terms of alterations in intrinsic organization^{29,73}. When coupled with theoretical studies using computational approaches similar to those reviewed here, such empirical studies have the potential to move beyond simply characterizing cognitive dysfunction, and to explain why there is a dysfunction from the perspective of brain network operation.

The empirical and computational studies of resting-state activity that we have reviewed in this article emphasize the importance of spontaneous activity for brain organization, and that this spontaneous activity cannot be modelled as purely random noise. Rather, the intrinsic architecture of the brain is organized in sets of discrete functional networks that are coherent at rest. Interestingly, some of these networks are organized as statistically independent dynamical systems, with high activity and coherence within one network corresponding to low activity and coherence within another network (a phenomenon known as anticorrelation). Furthermore, the emphasis on anatomical connectivity, noise and the space–time structure of network dynamics in our Review provides a framework that can guide future research and provides scientists with a new way of thinking about the brain's intrinsic functional architecture.

- Pinneo, L. R. On noise in the nervous system. *Psychol. Rev.* **73**, 242–247 (1966).
- An important paper in the archives of science that provides a compelling rationale for considering intrinsic activity as a vital part of brain function.
- Andreasen, N. C. *et al.* Remembering the past: two facets of episodic memory explored with positron emission tomography. *Am. J. Psychiatry* **152**, 1576–1585 (1995).
- Nyberg, L. *et al.* Network analysis of positron emission tomography regional cerebral blood flow data: ensemble inhibition during episodic memory retrieval. *J. Neurosci.* **16**, 3753–3759 (1996).
- Shulman, G. L. *et al.* Common blood flow changes across visual tasks: II. Decreases in cerebral cortex. *J. Cogn. Neurosci.* **9**, 648–663 (1997).
- Raichle, M. E. *et al.* A default mode of brain function. *Proc. Natl. Acad. Sci. USA* **98**, 676–682 (2001).
- The first complete articulation of the idea of a default mode of brain function based on both positron emission tomography (PET) blood flow studies and fMRI. This paper provided the framework for the study of intrinsic activity in neuroimaging.
- Fair, D. A. *et al.* The maturing architecture of the brain's default network. *Proc. Natl. Acad. Sci. USA* **105**, 4028–4032 (2008).
- Fransson, P. Spontaneous low-frequency BOLD signal fluctuations: an fMRI investigation of the resting-state default mode of brain function hypothesis. *Hum. Brain Mapp.* **26**, 15–29 (2005).
- Christoff, K., Gordon, A. M., Smallwood, J., Smith, R. & Schooler, J. W. Experience sampling during fMRI reveals default network and executive system contributions to mind wandering. *Proc. Natl. Acad. Sci. USA* **106**, 8719–8724 (2009).
- Christoff, K. *et al.* Rostrolateral prefrontal cortex involvement in relational integration during reasoning. *Neuroimage* **14**, 1136–1149 (2001).
- Vincent, J. L. *et al.* Intrinsic functional architecture in the anaesthetized monkey brain. *Nature* **447**, 83–86 (2007).
- This paper showed that resting-state networks correspond to functional networks that are activated under specific task or stimulation conditions, and suggested a strong relationship between the underlying neuroanatomical connectivity and the resting-state patterns.
- Fukunaga, M. *et al.* Large-amplitude, spatially correlated fluctuations in BOLD fMRI signals during extended rest and early sleep stages. *Magn. Reson. Imaging* **24**, 979–992 (2006).
- Horovitz, S. G. *et al.* Low frequency BOLD fluctuations during resting wakefulness and light sleep: a simultaneous EEG–fMRI study. *Hum. Brain Mapp.* **29**, 671–682 (2008).
- Picchioni, D. *et al.* fMRI differences between early and late stage-1 sleep. *Neurosci. Lett.* **441**, 81–85 (2008).
- D'Esposito, M., Ballard, D., Aguirre, G. K. & Zarahn, E. Human prefrontal cortex is not specific for working memory: a functional MRI study. *Neuroimage* **8**, 274–282 (1998).
- Poldrack, R. A. Can cognitive processes be inferred from neuroimaging data? *Trends Cogn. Sci.* **10**, 59–63 (2006).
- McIntosh, A. R. Towards a network theory of cognition. *Neural Netw.* **13**, 861–876 (2000).
- McIntosh, A. R. Contexts and catalysts: a resolution of the localization and integration of function in the brain. *Neuroinformatics* **2**, 175–182 (2004).

18. Biswal, B., Yetkin, F. Z., Haughton, V. M. & Hyde, J. S. Functional connectivity in the motor cortex of resting human brain using echo-planar MRI. *Magn. Reson. Med.* **34**, 537–541 (1995).
This paper demonstrated that brain regions that activate jointly seem to maintain a high correlation of BOLD signal fluctuations at rest, identifying a ‘resting-state network’ of ‘functionally connected’ regions. The paper’s method of analysis is now known as functional connectivity-by-MRI (fcMRI) or resting-state fMRI.
19. Greicius, M. D., Krasnow, B., Reiss, A. L. & Menon, V. Functional connectivity in the resting brain: a network analysis of the default mode hypothesis. *Proc. Natl Acad. Sci. USA* **100**, 253–258 (2003).
This paper studied for the first time the resting-state connectivity analysis of the default mode and provided clear evidence for the existence of a cohesive default mode network. It also investigated how the default mode network is modulated by task demands and what functions it might serve.
20. Lowe, M. J., Mock, B. J. & Sorenson, J. A. Functional connectivity in single and multislice echoplanar imaging using resting-state fluctuations. *Neuroimage* **7**, 119–132 (1998).
21. Rogers, B. P., Morgan, V. L., Newton, A. T. & Gore, J. C. Assessing functional connectivity in the human brain by fMRI. *Magn. Reson. Imaging* **25**, 1347–1357 (2007).
22. Damoiseaux, J. S. *et al.* Consistent resting-state networks across healthy subjects. *Proc. Natl Acad. Sci. USA* **103**, 13848–13853 (2006).
23. Fox, M. D. *et al.* The human brain is intrinsically organized into dynamic, anticorrelated functional networks. *Proc. Natl Acad. Sci. USA* **102**, 9673–9678 (2005).
This work was a compelling demonstration of at least two intrinsically coherent networks that could be captured using resting-state fMRI. The work led to the characterization as a task-positive and task-negative network, the latter corresponding to the default mode network
24. Fox, M. D., Zhang, D., Snyder, A. Z. & Raichle, M. E. The global signal and observed anticorrelated resting state brain networks. *J. Neurophysiol.* **101**, 3270–3283 (2009).
This paper investigated the anticorrelation between different resting-state networks, showing how the level of anticorrelation is affected by global signal removal. However, the authors demonstrated that several characteristics of anticorrelated networks are not attributable to global signal removal, suggesting that they have a biological basis.
25. Murphy, K., Birn, R. M., Handwerker, D. A., Jones, T. B. & Bandettini, P. A. The impact of global signal regression on resting state correlations: are anti-correlated networks introduced? *Neuroimage* **44**, 893–905 (2009).
26. Damoiseaux, J. S. *et al.* Reduced resting-state brain activity in the “default network” in normal aging. *Cereb. Cortex* **18**, 1856–1864 (2007).
27. Garrity, A. G. *et al.* Aberrant ‘default mode’ functional connectivity in schizophrenia. *Am. J. Psychiatry* **164**, 450–457 (2007).
28. Greicius, M. Resting-state functional connectivity in neuropsychiatric disorders. *Curr. Opin. Neurol.* **21**, 424–430 (2008).
This paper discusses how resting-state networks are disrupted in disorders in which cognition is also affected.
29. Rombouts, S. A. *et al.* Model-free group analysis shows altered BOLD fMRI networks in dementia. *Hum. Brain Mapp.* **30**, 256–266 (2009).
30. Hagmann, P. *et al.* Mapping the structural core of human cerebral cortex. *PLoS Biol.* **6**, e159 (2008).
31. Bullmore, E. & Sporns, O. Complex brain networks: graph theoretical analysis of structural and functional systems. *Nature Rev. Neurosci.* **10**, 186–198 (2009).
This is a comprehensive review of the principles of graph theory as they relate to brain networks. The empirical demonstrations are helpful in translating the measures to concrete applications.
32. Sporns, O. & Zwi, J. D. The small world of the cerebral cortex. *Neuroinformatics* **2**, 145–162 (2004).
33. Greicius, M. D., Supekar, K., Menon, V. & Dougherty, R. F. Resting-state functional connectivity reflects structural connectivity in the default mode network. *Cereb. Cortex* **19**, 72–78 (2009).
34. Honey, C. J. *et al.* Predicting human resting-state functional connectivity from structural connectivity. *Proc. Natl Acad. Sci. USA* **106**, 2035–2040 (2009). This paper used computational methods to compare anatomical and fMRI connectivity in humans. The authors concluded that the large-scale anatomical structure of the human cerebral cortex may constrain, but does not entirely account for, the observed global functional connectivity.
35. Koch, M. A., Norris, D. G. & Hund-Georgiadis, M. An investigation of functional and anatomical connectivity using magnetic resonance imaging. *Neuroimage* **16**, 241–250 (2002).
36. Honey, C. J., Kotter, R., Breakspear, M. & Sporns, O. Network structure of cerebral cortex shapes functional connectivity on multiple time scales. *Proc. Natl Acad. Sci. USA* **104**, 10240–10245 (2007).
37. Ghosh, A., Rho, Y., McIntosh, A. R., Kotter, R. & Jirsa, V. K. Noise during rest enables the exploration of the brain’s dynamic repertoire. *PLoS Comput. Biol.* **4**, e1000196 (2008).
This paper proposed that the space–time structure of coupling and time delays in the presence of noise define a dynamic framework for the emergence of activity fluctuations in the resting brain. It showed that fluctuations destabilize the ground state, producing excursion in the dynamical repertoire of the global brain network that results in oscillations structured in the experimentally observed resting-state subnetworks.
38. Deco, G., Jirsa, V., McIntosh, A. R., Sporns, O. & Kotter, R. Key role of coupling, delay, and noise in resting brain fluctuations. *Proc. Natl Acad. Sci. USA* **106**, 10302–10307 (2009).
This paper considered that resting-state ultraslow oscillations, and in particular the emergence of anticorrelated subnetworks, result from fluctuation-driven transitions between multistable states. Here, multistable cluster synchronization states appear in coupled oscillator systems owing to the delay of transmission times, highlighting the importance of the space–time structure of couplings in networks.
39. Valdes-Sosa, P. A. *et al.* Model driven EEG/fMRI fusion of brain oscillations. *Hum. Brain Mapp.* **30**, 2701–2721 (2009).
40. Bojak, I., Oostendorp, T. F., Reid, A. T. & Kotter, R. Connecting mean field models of neural activity to EEG and fMRI data. *Brain Topogr.* **23**, 139–149 (2010).
41. Izhikevich, E. M. & Edelman, G. M. Large-scale model of mammalian thalamocortical systems. *Proc. Natl Acad. Sci. USA* **105**, 3593–3598 (2008).
42. Hlinka, J. & Coombes, S. Depolarization induced suppression of excitation and the emergence of ultraslow rhythms in neural networks. *Phys. Rev. Lett.* **104**, 068101 (2010).
43. Steyn-Ross, D. A. & Steyn-Ross, M. (eds) *Modeling Phase Transitions in the Brain* (Springer, 2010).
44. Kotter, R. Online retrieval, processing, and visualization of primate connectivity data from the CoCoMac database. *Neuroinformatics* **2**, 127–144 (2004).
45. Stephan, K. E. *et al.* Advanced database methodology for the Collation of Connectivity data on the Macaque brain (CoCoMac). *Phil. Trans. R. Soc. Lond. B* **356**, 1159–1186 (2001).
46. Kotter, R. & Wanke, E. Mapping brains without coordinates. *Phil. Trans. R. Soc. Lond. B* **360**, 751–766 (2005).
47. Friston, K. J., Mechelli, A., Turner, R. & Price, C. J. Nonlinear responses in fMRI: the Balloon model, Volterra kernels, and other hemodynamics. *Neuroimage* **12**, 466–477 (2000).
48. Tzourio-Mazoyer, N. *et al.* Automated anatomical labeling of activations in SPM using a macroscopic anatomical parcellation of the MNI MRI single-subject brain. *Neuroimage* **15**, 273–289 (2002).
49. Monto, S., Palva, S., Voipio, J. & Palva, J. M. Very slow EEG fluctuations predict the dynamics of stimulus detection and oscillation amplitudes in humans. *J. Neurosci.* **28**, 8268–8272 (2008).
50. Nir, Y. *et al.* Interhemispheric correlations of slow spontaneous neuronal fluctuations revealed in human sensory cortex. *Nature Neurosci.* **11**, 1100–1108 (2008).
51. McNamara, B. & Wiesenfeld, K. Theory of stochastic resonance. *Phys. Rev. A* **39**, 4854–4869 (1989).
52. Chawla, D., Lumer, E. D. & Friston, K. J. Relating macroscopic measures of brain activity to fast, dynamic neuronal interactions. *Neural Comput.* **12**, 2805–2821 (2000).
53. Chawla, D., Lumer, E. D. & Friston, K. J. The relationship between synchronization among neuronal populations and their mean activity levels. *Neural Comput.* **11**, 1389–1411 (1999).
54. Zemanová, L., Zhou, C. & Kurths, J. Structural and functional clusters of complex brain networks. *Physica D* **224**, 202–212 (2006).
55. Zhou, C., Zemanová, L., Zamora, G., Hilgetag, C. C. & Kurths, J. Hierarchical organization unveiled by functional connectivity in complex brain networks. *Phys. Rev. Lett.* **97**, 238103 (2006).
56. Zhou, Y. *et al.* Functional dysconnectivity of the dorsolateral prefrontal cortex in first-episode schizophrenia using resting-state fMRI. *Neurosci. Lett.* **417**, 297–302 (2007).
57. Acerbon, J. A., Bonilla, L. L., Perez Vicente, C. J., Ritort, F. & Spigler, R. The Kuramoto model: a simple paradigm for synchronization phenomena. *Rev. Mod. Phys.* **77**, 137–185 (2005).
58. Kuramoto, Y. in *Lecture Notes in Physics* (ed. Araki, H.) 420 (Springer, New York, 1975).
59. Kenet, T., Bibitchkov, D., Tsodyks, M., Grinvald, A. & Arieli, A. Spontaneously emerging cortical representations of visual attributes. *Nature* **425**, 954–956 (2003).
60. Arieli, A., Sterkin, A., Grinvald, A. & Aertsen, A. Dynamics of ongoing activity: explanation of the large variability in evoked cortical responses. *Science* **273**, 1868–1871 (1996).
This study used optical imaging in the cat visual cortex to characterize the dynamics of spontaneous activity at rest. It showed that the variability of stimulus-evoked activity is largely accounted for by variation in spontaneous activity.
61. Blumenfeld, B., Bibitchkov, D. & Tsodyks, M. Neural network model of the primary visual cortex: from functional architecture to lateral connectivity and back. *J. Comput. Neurosci.* **20**, 219–241 (2006).
62. Muller-Linow, M., Hilgetag, C. C. & Hutt, M. T. Organization of excitatory dynamics in hierarchical biological networks. *PLoS Comput. Biol.* **4**, e1000190 (2008).
63. Lippe, S., Kovacevic, N. & McIntosh, A. R. Differential maturation of brain signal complexity in the human auditory and visual system. *Front. Hum. Neurosci.* **3**, 48 (2009).
64. McIntosh, A. R., Kovacevic, N. & Itier, R. J. Increased brain signal variability accompanies lower behavioral variability in development. *PLoS Comput. Biol.* **4**, e1000106 (2008).
65. Garrett, D. D., Kovacevic, N., McIntosh, A. R. & Grady, C. L. Blood oxygen level-dependent signal variability is more than just noise. *J. Neurosci.* **30**, 4914–4921 (2010).
66. Fox, M. D., Snyder, A. Z., Zacks, J. M. & Raichle, M. E. Coherent spontaneous activity accounts for trial-to-trial variability in human evoked brain responses. *Nature Neurosci.* **9**, 23–25 (2006).
This paper demonstrated that coherent spontaneous fluctuations in human brain activity account for a substantial fraction of the variability in measured event-related BOLD responses, and that spontaneous and task-related activity are linearly superimposed in the human brain.
67. Vincent, J. L. *et al.* Coherent spontaneous activity identifies a hippocampal-parietal memory network. *J. Neurophysiol.* **96**, 3517–3531 (2006).
68. Faisal, A. A., Selen, L. P. & Wolpert, D. M. Noise in the nervous system. *Nature Rev. Neurosci.* **9**, 292–303 (2008).
69. Knill, D. C. & Pouget, A. The Bayesian brain: the role of uncertainty in neural coding and computation. *Trends Neurosci.* **27**, 712–719 (2004).
70. Pouget, A., Dayan, P. & Zemel, R. S. Inference and computation with population codes. *Annu. Rev. Neurosci.* **26**, 381–410 (2003).
71. Mantini, D., Perrucci, M. G., Del Gratta, C., Romani, G. L. & Corbetta, M. Electrophysiological signatures of resting state networks in the human brain. *Proc. Natl Acad. Sci. USA* **104**, 13170–13175 (2007).
72. Gao, W. *et al.* Evidence on the emergence of the brain’s default network from 2-week-old to 2-year-old healthy pediatric subjects. *Proc. Natl Acad. Sci. USA* **106**, 6790–6795 (2009).
73. Grady, C. L. *et al.* A multivariate analysis of age-related differences in default mode and task-positive networks across multiple cognitive domains. *Cereb. Cortex* **20**, 1432–1447 (2009).
74. Jirsa, V. K. & Haken, H. Field theory of electromagnetic brain activity. *Phys. Rev. Lett.* **77**, 960–963 (1996).

75. Jirsa, V. K. & Haken, H. A derivation of a macroscopic field theory of the brain from the quasi-microscopic neural dynamics. *Physica D* **99**, 503–526 (1997).
76. Robinson, P. A., Rennie, C. J. & Wright, J. J. Propagation and stability of waves of electrical activity in the cerebral cortex. *Phys. Rev. E* **56**, 826–840 (1997).
77. Breakspear, M. *et al.* A unifying explanation of primary generalized seizures through nonlinear brain modeling and bifurcation analysis. *Cereb. Cortex* **16**, 1296–1313 (2006).
78. Nunez, P. L. The brain wave equation: a model for the EEG. *Math. Biosci.* **21**, 279–297 (1974).
79. Rodriguesz, S., Terry, J. R. & Breakspear, M. On the genesis of spike-wave oscillations in a mean-field model of human corticothalamic dynamics. *Phys. Lett. A* **355**, 352–357 (2006).
80. Horwitz, B. & Husain, F. T. in *Handbook on Brain Connectivity* (eds Jirsa, V. K. & McIntosh, A. R.) 275–302 (Springer, New York, 2007).
81. Tuckwell, H. C. *Introduction to Theoretical Neurobiology* (Cambridge Univ. Press, 1988).
82. Knight, B. W., Omurtag, A. & Sirovich, L. The approach of a neuron population firing rate to a new equilibrium: an exact theoretical result. *Neural Comput.* **12**, 1045–1055 (2000).
83. Wilson, H. R. & Cowan, J. D. Excitatory and inhibitory interactions in localized populations of model neurons. *Biophys. J.* **12**, 1–24 (1972).
84. Assisi, C. G., Jirsa, V. K. & Kelso, J. A. Synchrony and clustering in heterogeneous networks with global coupling and parameter dispersion. *Phys. Rev. Lett.* **94**, 018106 (2005).
85. Stefanescu, R. A. & Jirsa, V. K. A low dimensional description of globally coupled heterogeneous neural networks of excitatory and inhibitory neurons. *PLoS Comput. Biol.* **4**, e1000219 (2008).

Acknowledgements

We are grateful for funding received from the James S. McDonnell Foundation (grant Brain NRG [JSMF22002082]).

Competing interests statement

The authors declare no competing financial interests.

FURTHER INFORMATION

Gustavo Deco's homepage: <http://cns.upf.edu/index.html>

Viktor K. Jirsa's homepage: <http://www.ism.univmed.fr>

Anthony R. McIntosh's homepage: www.rotman-baycrest.on.ca/index.php?section=211

ALL LINKS ARE ACTIVE IN THE ONLINE PDF